Input-Output Linearization of MIMO Systems with Applications to Longitudinal Flight Dynamics

Jhon Manuel Portella Delgado and Ankit Goel

***Abstract*— This paper presents an extension of the input-output linearization method for nonsquare systems with more outputs than inputs. Unlike the square systems and nonsquare systems with fewer outputs than inputs, which can be completely linearized, we consider the problem of linearizing nonsquare systems with more outputs than inputs. In particular, the system is linearized by decomposing the state using a diffeomorphism, which is chosen such that the output of the system is a linear combination of the outputs of integrator chains, and the input of the system is chosen to cancel the nonlinearities using feedback linearization. In the case of nonsquare systems with more outputs than inputs, we observe that the resulting linear system can be stabilized even though it is uncontrollable at all times. This apparent contradiction is due to the switching behavior in the control action. We apply the input-output linearization method to linearize the longitudinal aircraft dynamics and demonstrate asymptotic stability of the closed-loop system despite the switching behavior.**

I. INTRODUCTION

Although input-output linearization methods have been well-studied for square systems and nonsquare systems with fewer outputs than inputs, these methods have not been explored for system with more outputs than inputs [1]–[4]. In the classical input-output linearization method, a diffeomorphism is used to transform the state such that the dynamics matrix of a part of the transformed state is in the Jordan form, whereas the input matrix potentially remains a nonlinear function of the full state [3]. It turns out that, in the case of square systems and nonsquare systems with fewer outputs than inputs, the transformed input matrix, which is square or wide, is often full-column rank. Nonlinearities thus can be canceled exactly to yield a linear input-output system. On the other hand, in the case of nonsquare systems with more outputs than inputs, the transformed input matrix, which is tall, does not yield a fully controllable linear input-output system. In this paper, we extend the input-output linearization method for such systems.

Jhon Manuel Portella Delgado is a graduate student in the Department of Mechanical Engineering, University of Maryland, Baltimore County, 1000 Hilltop Circle, Baltimore, MD 21250. jportel1@umbc.edu

Ankit Goel is an Assistant Professor in the Department of Mechanical Engineering, University of Maryland, Baltimore County,1000 Hilltop Circle, Baltimore, MD 21250. ankgoel@umbc.edu

This extension is motivated by the problem of linearizing the longitudinal aircraft dynamics. The longitudinal dynamics of an aircraft typically has two inputs, namely thrust and the elevator-deflection angle and two outputs, namely the velocity and the flight-path angle [5], [6]. Although this square system can be linearized by input-output linearization methods, the resulting zero dynamics turns out to be unstable. We show, in this paper, that the zero dynamics can be eliminated by considering an additional output in the linearization process. However, the resulting linearized system turns out to be uncontrollable at all time. Nonetheless, we observe that, even though the resulting linear system is uncontrollable, the uncontrollable modes are not fixed in time. In fact, the uncontrollable modes switch as a function of the state, which allows the state of the system to be driven to zero.

Several methods have been explored to regulate the states of aircraft longitudinal dynamics. The total energy control system proposed in [7], [8] transforms the states to energy states and uses heuristically tuned PID gains to regulate the states of the aircraft. However, this approach does not guarantee stability of the closed-loop system. Nonlinear backstepping methods have also been investigated to solve this problem [9]. Since backstepping methods require the dynamics to be in a strict feedback form, these approaches often omit the effect of the elevator deflection on the lift in order to formulate the dynamics in strict feedback form. This paper considers a more realistic model of an aircraft by including the effect of the elevator deflection on the lift. Since the dynamics considered in this paper is not in a strict feedback form, classical backstepping methods are not applicable.

In order to regulate the longitudinal aircraft dynamics with theoretical guarantees, this paper extends the input-output linearization method to the case of nonsquare systems with more outputs than inputs, and applies it to design a controller to linearizing the aircraft longitudinal dynamics. The paper is organized as follows. Section II describes the problem considered in this paper and reviews relevant definitions, Section III presents the input-output linearization method for under-actuated MIMO systems, Section IV describes the longitudinal aircraft dynamics used to construct the input-output linearizing controller, Section V shows the application of the input-output linearization method to the problem of linearizing longitudinal aircraft dynamics in the case of two and three outputs, and Section VI shows the results of the numerical simulations of the closed-loop longitudinal aircraft dynamics. Finally, the paper concludes with a discussion of results and future research directions in Section VII.

II. Problem Formulation

Consider an affine system

$$\dot{x} = f(x) + g(x)u, \tag{1}$$
$$y = h(x), \tag{2}$$

where $x(t) \in \mathbb{R}^{l_x}$ is the state, $u(t) \in \mathbb{R}^{l_u}$ is the input, $y(t) \in \mathbb{R}^{l_y}$ is the output, and f, g, h are smooth functions of appropriate dimensions. The objective is to construct a control law such the dynamics from the input to the output is linear, that is,

$$\dot{\xi} = A\xi + Bv, \tag{3}$$
$$y = C\xi, \tag{4}$$

where A, B, C are, possibly user-defined, known matrices, ξ, not necessarily equal to x, is a state, and v is the control which can be designed to obtain any desired output response using tools from linear systems theory.

The following definitions appear in [4] and are repeated here for further use in the paper.

Definition 2.1: In the system (1), (2). the relative degree of the ith output y_i is the smallest integer $\rho_i \geq 0$ such that ρ_i-th derivative of y_i, that is $y_i^{(\rho_i)}$, is an explicit function of input u.

Definition 2.2: The relative degree of the system (1), (2) is the sum of the relative degree of each of its outputs, that is, $\rho \triangleq \sum_i^{l_y} \rho_i$.

III. MIMO Input-Output Linearization

This section reviews the multi-input, multi-output extension of the input-output linearizing control presented in [1], and extends it to the case of nonsquare systems with more outputs than inputs..

Consider the transformation

$$T : \mathbb{R}^{l_x} \to \mathbb{R}^{l_x}$$
$$T(x) = \begin{bmatrix} \phi(x) \\ \psi(x) \end{bmatrix}, \tag{5}$$

where $\phi(x)$ satisfies

$$L_g \phi(x) = 0, \tag{6}$$

and

$$\psi(x) = \begin{bmatrix} \psi_1(x) \\ \vdots \\ \psi_{l_y}(x) \end{bmatrix}, \tag{7}$$

where

$$\psi_i(x) \triangleq \begin{bmatrix} h_i(x) \\ L_f h_i(x) \\ \vdots \\ L_f^{\rho_i - 1} h_i(x) \end{bmatrix} \in \mathbb{R}^{\rho_i}. \tag{8}$$

Note that $\phi : \mathbb{R}^{l_x} \to \mathbb{R}^{l_x - \rho}$ and, for $i = 1, \ldots, l_y$, $\psi_i : \mathbb{R}^{l_x} \to \mathbb{R}^{\rho_i}$, and thus $\psi : \mathbb{R}^{l_x} \to \mathbb{R}^{\rho}$. Furthermore, the functions ψ_i are well-defined since the functions f, g, h are assumed to be smooth. However, ϕ satisfying (6) may or may not exist.

Assuming that ϕ satisfying (6) exists and defining $\eta \triangleq \phi(x)$, it follows that

$$\dot{\eta} = L_f \phi(x) + L_g \phi(x) u = L_f \phi(x), \tag{9}$$

where $L_g \phi(x) = 0$ by construction. Note that (9) is the *zero dynamics* [3].

Next, defining $\xi \triangleq \psi(x)$, it follows that

$$\dot{\xi} = L_f \psi(x) + L_g \psi(x) u. \tag{10}$$

Next, note that

$$L_f \psi(x) = A_{\rm c} \xi + B_{\rm c} \begin{bmatrix} L_f^{\rho_1} h_1(x) \\ \vdots \\ L_f^{\rho_{l_y}} h_{l_y}(x) \end{bmatrix}, \tag{11}$$

where $A_{\rm c} = \operatorname{diag}(A_{{\rm c},1}, \ldots, A_{{\rm c},l_y}) \in \mathbb{R}^{\rho \times \rho}$ and $B_{\rm c} = \operatorname{diag}(b_{{\rm c},1}, \ldots, b_{{\rm c},l_y}) \in \mathbb{R}^{\rho \times l_y}$ and, for $i = 1, \ldots, l_y$,

$$A_{{\rm c},i} \triangleq \begin{bmatrix} 0 & 1 & 0 & \cdots & 0 \\ 0 & 0 & 1 & \cdots & 0 \\ \vdots & \vdots & \ddots & \ddots & \vdots \\ 0 & \cdots & \cdots & 0 & 1 \\ 0 & \cdots & \cdots & 0 & 0 \end{bmatrix} \in \mathbb{R}^{\rho_i \times \rho_i}, \tag{12}$$

$$b_{{\rm c},i} \triangleq \begin{bmatrix} 0 \\ \vdots \\ 1 \end{bmatrix} \in \mathbb{R}^{\rho_i}. \tag{13}$$

Finally,

$$L_g \psi(x) = B_{\rm c} \begin{bmatrix} L_g L_f^{\rho_i - 1} h_1(x) \\ \vdots \\ L_g L_f^{\rho_{l_y} - 1} h_{l_y}(x) \end{bmatrix}. \tag{14}$$

Substituting (11) and (14) in (10) yields

$$\dot{\xi} = A_{\rm c} \xi + B_{\rm c} \gamma(x)[u - \alpha(x)], \tag{15}$$

where

$$\gamma(x) \triangleq \begin{bmatrix} L_g L_f^{\rho_i-1} h_1(x) \\ \vdots \\ L_g L_f^{\rho_{l_y}-1} h_{l_y}(x) \end{bmatrix} \in \mathbb{R}^{l_y \times l_u}, \tag{16}$$

$$\alpha(x) \triangleq \gamma(x)^+ \begin{bmatrix} -L_f^{\rho_1} h_1(x) \\ \vdots \\ -L_f^{\rho_{l_y}} h_{l_y}(x) \end{bmatrix} \in \mathbb{R}^{l_u}. \tag{17}$$

where $\gamma(x)^+ \in \mathbb{R}^{l_u \times l_y}$ is the psuedo-inverse of $\gamma(x)$. Finally, letting

$$u(x) = \alpha(x) + \gamma(x)^+ v, \tag{18}$$

yields

$$\dot{\xi} = A_c \xi + B_c \Lambda(x) v, \tag{19}$$

where $\Lambda(x) \triangleq \gamma(x)\gamma(x)^+ \in \mathbb{R}^{l_y \times l_y}$ and $v \in \mathbb{R}^{l_y}$. Note that

$$\Lambda(x) = \begin{bmatrix} \lambda_1(x) & \cdots & 0 \\ \vdots & \ddots & \vdots \\ 0 & \cdots & \lambda_{l_y}(x) \end{bmatrix}, \tag{20}$$

where, for all $i = 1, \ldots, l_y$, $\lambda_i(x)$ is either 1 or 0. Note that (18) is the *input-output linearizing* (IOL) controller and (19) is the linearized system.

In the square and wide plants, where $l_u \geq l_y$, if $\gamma(x)$ is full-column rank for all x, then, for all $i = 1, \ldots, l_y$, $\lambda_i(x) = 1$, and thus $\Lambda(x) = I_{l_y}$. Consequently, all of the outputs can be directly manipulated by appropriately defining the control signal v.

On the other hand, in the tall plants, where $l_u < l_y$, at least $l_y - l_u$ diagonal elements of $\Lambda(x)$ are zero. Furthermore, if $\gamma(x)$ is full-column rank for all x, then exactly $l_y - l_u$ diagonal elements of $\Lambda(x)$ are zero. However, it is not necessary that a particular $\lambda_i(x)$ is always zero. Each $\lambda_i(x)$ may switch between 0 and 1, giving rise to a *switched input system*. As shown in the numerical example considered later in the paper, this input-switching property allows full manipulation of the state ξ even though $\Lambda(x)$ is not full rank.

IV. Longitudinal Aircraft Dynamics

This section reviews the longitudinal dynamics of an aircraft and presents the notation used in this paper. The longitudinal flight dynamics are given by

$$\dot{V} = \frac{1}{m}[F\cos(\alpha) - D - mg\sin(\gamma)], \tag{21}$$

$$\dot{\gamma} = \frac{1}{mV}[F\sin(\alpha) + L - mg\cos(\gamma)], \tag{22}$$

$$\dot{\theta} = q \tag{23}$$

$$\dot{q} = \frac{M}{I_{yy}}, \tag{24}$$

where V in the velocity, γ is the flight-path angle, θ is the pitch angle, $\alpha \triangleq \theta - \gamma$ is the angle-of-attack, q is the pitch rate, F is the thrust, and $\delta_{\rm e}$ is the elevator deflection angle. [10]. The lift L, the drag D, and the moment M are parameterized as

$$L = \frac{1}{2}\rho V^2 S C_{\rm L}, \tag{25}$$

$$D = \frac{1}{2}\rho V^2 S C_{\rm D}, \tag{26}$$

$$M = \frac{1}{2}\rho V^2 S \overline{c} C_{\rm M}, \tag{27}$$

where ρ is the air density, S is the wing surface area, and $\overline{c}$ is the mean chord length. Finally, the lift coefficient $C_{\rm L}$, the draf coefficient $C_{\rm D}$, and the moment coefficient $C_{\rm M}$ are parameterized as

$$C_{\rm L} = C_{\rm L_0} + C_{\rm L_\alpha}\alpha + C_{\rm L_{\delta_e}}\delta_e, \tag{28}$$

$$C_{\rm D} = C_{D_0} + C_{D_\alpha}\alpha, \tag{29}$$

$$C_{\rm M} = C_{m_0} + C_{m_\alpha}\alpha + C_{m\delta_{\rm e}}\delta_{\rm e}, \tag{30}$$

where $C_{D_0}, C_{D_\alpha}, C_{\rm L_0}, C_{\rm L_\alpha}, C_{{\rm L}\delta_{\rm e}}, C_{m_0}, C_{m_\alpha}$, and $C_{m\delta_{\rm e}}$ are aircraft aerodynamic coefficients, and $\delta_{\rm e}$ is the elevator angle. Note that the inclusion of $C_{\rm L_{\delta_e}}$ in the dynamics makes the system non-triangular, and hence, conventional backstepping methods can not be applied to this problem [9].

V. Input-Output Linearization of Longitudinal Aircraft Dynamics

This section applies the input-output linearizing control presented in Section III to the longitudinal aircraft dynamics problem. In particular, we consider two cases. Since, tn typical longitudinal flight controllers, the velocity and flight-path angle references are given by an appropriate guidance law, in the first case, we construct a linearizing controller to drive the velocity error and the flight-path angle error to zero. However, it turns out that the corresponding zero dynamics in this case is unstable. Next, in order to remove the detrimental effect of the zero dynamics, we construct a linearizing controller to drive the velocity error, the flight-path angle error, and the pitch angle error to zero. In this case, it turns out that there is no zero dynamics. Note that we use the trim conditions to compute the desired pitch angle and the pitch angle error used by the linearizing controller.

A. Two outputs

Defining $x \triangleq \begin{bmatrix} V - \overline{V} & \gamma - \overline{\gamma} & \theta & q \end{bmatrix}^{\rm T}$ and $u \triangleq \begin{bmatrix} F & \delta_{\rm e} \end{bmatrix}^{\rm T}$, it follows that (21)-(24) can be written as

(1), (2), where

$$f_1(x) \triangleq -\frac{\rho(x_1+\overline{V})^2 S}{2m}(C_{D_0}+C_{D_\alpha}(x_3-x_2-\overline{\gamma})) - g\sin(x_2+\overline{\gamma}) - \dot{\overline{V}}, \tag{31}$$

$$f_2(x) \triangleq \frac{\rho(x_1+\overline{V})S}{2m}(C_{\mathrm{L}_0}+C_{\mathrm{L}_\alpha}(x_3-x_2-\overline{\gamma})) - \frac{g\cos(x_2+\overline{\gamma})}{(x_1+\overline{V})} - \dot{\overline{\gamma}}, \tag{32}$$

$$f_3(x) \triangleq x_4, \tag{33}$$

$$f_4(x) \triangleq \frac{\rho(x_1+\overline{V})S\overline{c}}{2I_{yy}}(C_{m_0}+C_{m_\alpha}(x_3-x_2-\overline{\gamma})), \tag{34}$$

and

$$g(x) = \begin{bmatrix} \frac{\cos(x_3-x_2-\overline{\gamma})}{m} & 0 \\ \frac{\sin(x_3-x_2-\overline{\gamma})}{m(x_1+\overline{V})} & \frac{\rho(x_1+\overline{V})S}{2m}C_{\mathrm{L}\delta_\mathrm{e}} \\ 0 & 0 \\ 0 & \frac{\rho(x_1+\overline{V})S\overline{c}}{2I_{yy}}C_{m\delta_\mathrm{e}} \end{bmatrix}. \tag{35}$$

It is assumed that $\overline{V}, \dot{\overline{V}}, \overline{\gamma}, \dot{\overline{\gamma}}$ are well-defined. The output y is given by

$$y = h(x) \triangleq \begin{bmatrix} x_1 \\ x_2 \end{bmatrix}. \tag{36}$$

Note that, in this formulation of the dynamics, x_1 is the velocity error and x_2 is the flight-path angle error.

Next, note that $\rho_1 = \rho_2 = 1$, and thus $\rho = 2$. This implies that the $\eta = \phi(x) \in \mathbb{R}^2$ and $\xi = \psi(x) \in \mathbb{R}^2$. It follows from (8) that

$$\xi_1 = x_1, \tag{37}$$

$$\xi_2 = x_2. \tag{38}$$

Furthermore,

$$\gamma(x) = \begin{bmatrix} \frac{\cos(x_3-x_2-\overline{\gamma})}{m} & 0 \\ \frac{\sin(x_3-x_2-\overline{\gamma})}{m(x_1+\overline{V})} & \frac{\rho(x_1+\overline{V})S}{2m}C_{L\delta_\mathrm{e}} \end{bmatrix}. \tag{39}$$

Note that, if $x_1 \neq -\overline{V}$ and $x_3 - x_2 - \overline{\gamma} \neq \frac{\pi}{2}$, then $\det(\gamma(x)) \neq 0$. and thus, the input-output linearizing control given by (18) yields

$$\dot{x}_1 = v_1, \tag{40}$$

$$\dot{x}_2 = v_2. \tag{41}$$

Next, solving (6) yields

$$\eta_1 = \sin(x_3-x_2-\overline{\gamma})(x_1+\overline{V}), \tag{42}$$

$$\eta_2 = \frac{m\overline{c}C_{m\delta_\mathrm{e}}}{I_{yy}C_{\mathrm{L}\delta_\mathrm{e}}}x_2 - x_4, \tag{43}$$

and thus the zero dynamics is given by

$$\dot{\eta}_1 = \eta_1\Bigg[-\frac{\rho\overline{V}S}{2m}\left(C_{D_0}+C_{D_\alpha}\arcsin\left(\frac{\eta_1}{\overline{V}}\right)\right) - \frac{g\sin\overline{\gamma}}{\overline{V}} - \frac{\dot{\overline{V}}}{\overline{V}}\Bigg] + \sqrt{(\overline{V}^2-\eta_1^2)}\Bigg[-\frac{\rho\overline{V}S}{2m}\left(C_{\mathrm{L}_0}+C_{\mathrm{L}_\alpha}\arcsin\left(\frac{\eta_1}{\overline{V}}\right)\right) + \frac{g\cos\overline{\gamma}}{\overline{V}} + \dot{\overline{\gamma}} - \eta_2\Bigg], \tag{44}$$

$$\dot{\eta}_2 = \frac{\rho\overline{V}S\overline{c}C_{m\delta_\mathrm{e}}}{2I_{yy}C_{\mathrm{L}\delta_\mathrm{e}}}\left(C_{\mathrm{L}_0}+C_{\mathrm{L}_\alpha}\arcsin\left(\frac{\eta_1}{\overline{V}}\right)\right) - \frac{mg\overline{c}C_{m\delta_\mathrm{e}}\cos\overline{\gamma}}{I_{yy}\overline{V}C_{\mathrm{L}\delta_\mathrm{e}}} - \frac{m\overline{c}C_{m\delta_\mathrm{e}}\dot{\overline{\gamma}}}{I_{yy}C_{\mathrm{L}\delta_\mathrm{e}}} - \frac{\rho\overline{V}S\overline{c}}{2I_{yy}}\left(C_{m_0}+C_{m_\alpha}\arcsin\left(\frac{\eta_1}{\overline{V}}\right)\right). \tag{45}$$

Several simulations with nominal values of the parameters show that the zero-dynamics in this case is in fact unstable. Furthermore, since

$$x_3 = \arcsin\left(\frac{\eta_1}{\xi_1+\overline{V}}\right) + \xi_2 + \overline{\gamma}, \tag{46}$$

$$x_4 = \frac{m\overline{c}C_{m\delta_\mathrm{e}}}{I_{yy}C_{\mathrm{L}\delta_\mathrm{e}}}\xi_2 - \eta_2, \tag{47}$$

the pitch angle and the pitch rate also diverge due to the unstable zero dynamics.

B. Three outputs

In order to remove the unstable zero dynamics, we consider an additional output, as shown below. In particular, we assume that the pitch angle of the aircraft is commanded to a desired value, which is assumed to be given by the desired trim condition. Redefining the state $x \triangleq \begin{bmatrix} V-\overline{V} & \gamma-\overline{\gamma} & \theta-\overline{\theta} & q \end{bmatrix}^\mathrm{T}$, it follows that

(21)-(24) can be written as (1), (2), where

$$f_1(x) \triangleq -\frac{\rho(x_1+\overline{V})^2 S}{2m}(C_{D_0}+C_{D_\alpha}(x_3+\overline{\theta}-x_2-\overline{\gamma})) - g\sin(x_2+\overline{\gamma}) - \dot{\overline{V}}, \tag{48}$$

$$f_2(x) \triangleq \frac{\rho(x_1+\overline{V})S}{2m}(C_{\mathrm{L}_0}+C_{\mathrm{L}_\alpha}(x_3+\overline{\theta}-x_2-\overline{\gamma})) - \frac{g\cos(x_2+\overline{\gamma})}{(x_1+\overline{V})} - \dot{\overline{\gamma}}, \tag{49}$$

$$f_3(x) \triangleq x_4, \tag{50}$$

$$f_4(x) \triangleq \frac{\rho(x_1+\overline{V})S\overline{c}}{2I_{yy}}(C_{m_0}+C_{m_\alpha}(x_3+\overline{\theta}-x_2-\overline{\gamma})) - \ddot{\overline{\theta}}. \tag{51}$$

The output y is given by

$$y = h(x) \triangleq \begin{bmatrix} x_1 \\ x_2 \\ x_3 \end{bmatrix}. \tag{52}$$

Note that the output now consists of the velocity error, the flight-path angle error, and the pitch-angle error.

Next, note that $\rho_1 = \rho_2 = 1$, and $\rho_3 = 2$, and thus $\rho = 4$ and thus $\xi = \psi(x) \in \mathbb{R}^4$. In fact, it follows from (7) and (8) that $\psi(x) = x$, and thus there is no zero dynamics. Finally, the input-output linearizing control is given by (18) with

$$\gamma(x) = \begin{bmatrix} \dfrac{\cos(x_3-x_2-\overline{\gamma})}{m} & 0 \\ \dfrac{\sin(x_3-x_2-\overline{\gamma})}{m(x_1+\overline{V})} & \dfrac{\rho(x_1+\overline{V})S}{2m}C_{L\delta_{\mathrm{e}}} \\ 0 & \dfrac{\rho(x_1+\overline{V})S\overline{c}}{2I_{yy}}C_{m\delta_{\mathrm{e}}} \end{bmatrix}, \tag{53}$$

and

$$\alpha(x) = -\gamma(x)^+ \begin{bmatrix} f_1(x) \\ f_2(x) \\ f_4(x) \end{bmatrix}. \tag{54}$$

The closed-loop system is thus

$$\dot{x} = A_{\mathrm{c}}x + B_{\mathrm{c}}\Lambda(x)v, \tag{55}$$

where

$$A_{\mathrm{c}} = \begin{bmatrix} 0&0&0&0\\0&0&0&0\\0&0&0&1\\0&0&0&0 \end{bmatrix}, B_{\mathrm{c}} = \begin{bmatrix} 1&0&0\\0&1&0\\0&0&0\\0&0&1 \end{bmatrix}, \tag{56}$$

Numerical simulations have revealed that

$$\Lambda(x) = \begin{bmatrix} \lambda_1(x) & 0 & 0 \\ 0 & \lambda_2(x) & 0 \\ 0 & 0 & 1 \end{bmatrix} \tag{57}$$

where $\lambda_1(x) \neq \lambda_2(x)$ are either 1 or 0. That is, if $\lambda_1(x) = 1$, then $\lambda_2(x) = 0$, and vice-versa.

This structure of the closed-loop dynamics (55) suggests that the pitch angle and the pitch rate is stabilized by the control law $v_3 = k_3x_3 + k_4x_4$, where $k_3, k_4 < 0$. The closed-loop dynamics also reveals the switching behaviour of the control action in the first two states, namely, the velocity error and the flight-path angle error, since the rank of $\Lambda(x) \in \mathbb{R}^{3\times 3}$ is 2. Letting $k_1, k_2 < 0$ yields

$$\dot{x}_1 = k_1\lambda_1(x)x_1, \tag{58}$$

$$\dot{x}_2 = k_2\lambda_2(x)x_2. \tag{59}$$

Note that x_1 and x_2 converge to 0 if $\lambda_1(x)$ and $\lambda_2(x)$ keep switching. Numerical example shown in the next section show that $\lambda_1(x)$ and $\lambda_2(x)$ indeed keep switching in this particular application, and thus the velocity error, flight-path error, and this pitch angle error converge to zero asymptotically.

VI. Simulation Results

This section demonstrates a numerical example of application of the input-output linearizing control to the Longitudinal flight dynamics. Consider the model of A330 given in [11]. The equilibrium inputs are obtained by numerically finding the roots of the dynamics equations. Figure 1 shows the equilibrium inputs required to maintain a steady-state at several velocities for the model used in this paper.

In order to demonstrate the application of the input-output linearizing controller, the aircraft is assumed to be flying at steady-state with a velocity of 200 m/s at an altitude of $10,000$ km. The aircraft is then commanded to increase its velocity to 250 m/s. The desired pitch angle is given by computing the equilibrium state for the chosen velocity. Letting $k_1 = -0.5, k_2 = -1, k_3 = -5, k_4 = -3$ Figure 2 shows the velocity, flight path angle, and the pitch of the aircraft and Figure 3 shows the control inputs given by the input-output linearizing controller. Figure 4 shows the switching behavior of the components of $\Lambda(x)$, that allows the state errors to converge to zero. Finally, Figure 5 shows the closed-loop response of the aircraft for several values of gains. Since the velocity and the flight-path angle states are independently controlled, their time response can be arbitrarily chosen by appropriately choosing k_1 and k_2, respectively. Similarly, an arbitrary pitch response can be obtained designed by appropriately choosing k_3 and k_4.

In this formulation of the input-output linearizing controller, reference value of the pitch angle is required to compute the control signal. In practice, however, the pitch angle at the desired trim condition can not be exactly determined. Nonetheless, the control signals can be computed with the incorrect pitch reference. Figure 6 shows the closed-loop response of the aircraft in this case. Note that, as expected, the the flight-path angle does not converge to zero and the pitch does not converge to the correct pitch reference, however, the velocity converges to the correct reference.

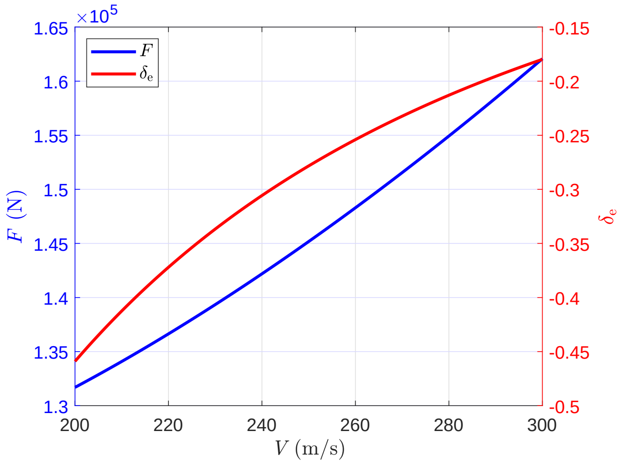

Fig. 1: Input values to maintain steady state at various aircraft velocities.

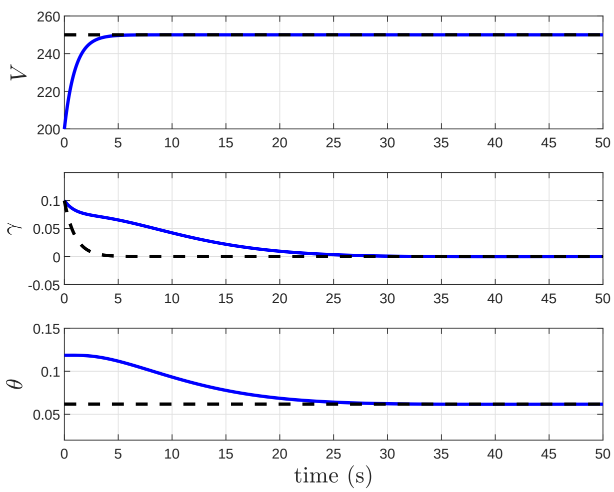

Fig. 2: Velocity, flight-path angle, and the pitch angle response of the linearized longitudinal aircraft dynamics. Note that the output is shown in solid blue and the corresponding reference is shown in dashed black.

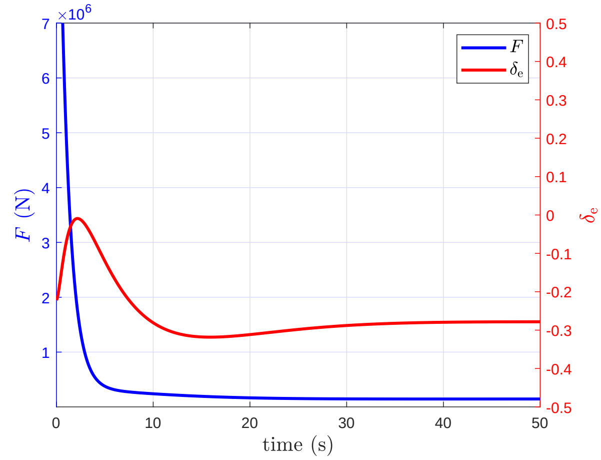

Fig. 3: Thrust and elevator-deflection angle given by the linearizing controller.

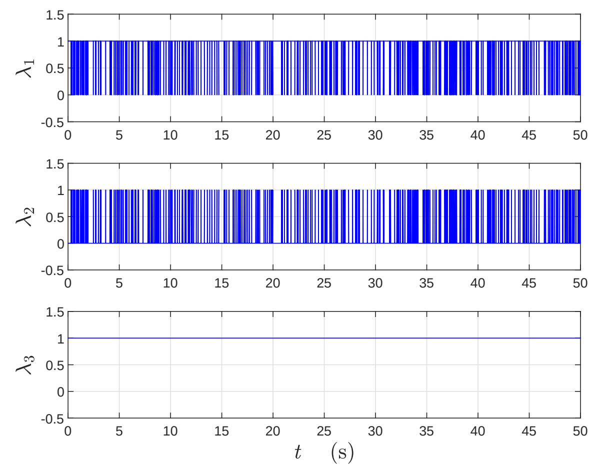

Fig. 4: The diagonal components of $\Lambda(x)$. Note that $\lambda_1(x)$ and $\lambda_1(x)$ switch between 0 and 1, whereas $\lambda_1(x) = 1$ for all $t \geq 0$. The switching behavior allows both the velocity error and the flight-path angle error to be driven to zero in spite of the fact that the rank of $\Lambda(x) = 2$ for all $t \geq 0$.

VII. Conclusions and Future Work

This paper presented an extension of the MIMO input-output linearization method applicable to under-actuated plants and applied the method to stabilize the longitudinal flight dynamics. The numerical simulations presented in the paper reveal that the application of the method to under-actuated plants leads to a switching behavior in the control action.

The future work will focus on the structure of the switching matrix $\Lambda(x)$ in order to develop theoretical guarantees for globally asymptotically stable controllers. In addition, we will focus on relaxing the assumptions including exact knowledge of the various coefficients parameterizing the dynamics as well as the exact knowledge of trim conditions. In particular, we will extend the method by including adaptive laws to estimate the coefficients online and use reference governor to update the setpoints.

References

[1] S. Kolavennu, S. Palanki, and J. C. Cockburn, “Nonlinear control of nonsquare multivariable systems,” *Chemical Engineering Science*, vol. 56, no. 6, pp. 2103–2110, 2001.

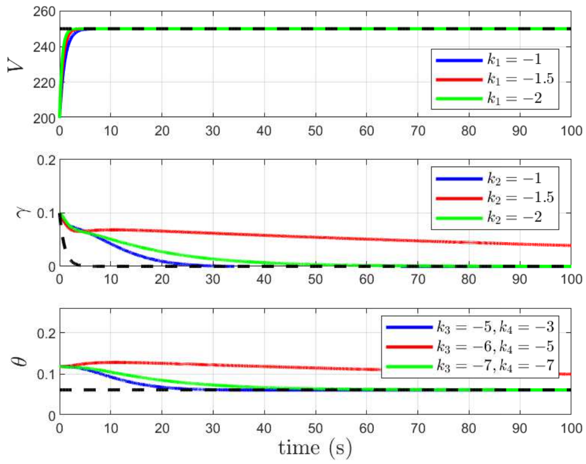

Fig. 5: Velocity, flight-path angle, and the pitch angle response of the linearized longitudinal aircraft dynamics for various values of the controller gains. Note that the time response of each state can be independently controlled by varying the value of the corresponding gain.

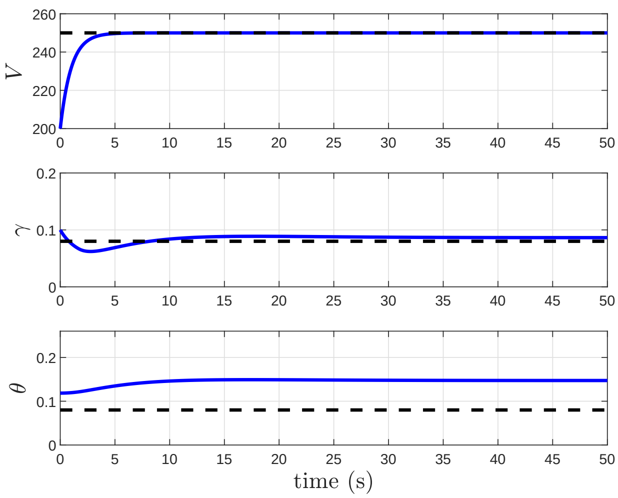

Fig. 6: Velocity, flight-path angle, and the pitch angle response of the linearized longitudinal aircraft dynamics with inconsistent pitch reference. Note that the inconsistent pitch reference cannot be attained by simultaneously driving the flight path angle to zero.

[2] K. S. D. Alharbi, *Backstepping Control and Transformation of Multi-Input Multi-Output Affine Nonlinear Systems into a Strict Feedback Form*. University of Arkansas, 2019.

[3] H. K. Khalil, *Nonlinear systems; 3rd ed.* Upper Saddle River, NJ: Prentice-Hall, 2002.

[4] A. Isidori, *Nonlinear control systems: an introduction*. Springer, 1985.

[5] B. Etkin and L. D. Reid, *Dynamics of flight. Stability and Control*, Third. John Wiley, 1996.

[6] B. L. Stevens, F. L. Lewis, and E. N. Johnson, *Aircraft control and simulation: dynamics, controls design, and autonomous systems*, Third. John Wiley, 2003.

[7] A. Lambregts, "Integrated system design for flight and propulsion control using total energy principles," in *Aircraft design, systems and technology meeting*, 1983, p. 2561.

[8] ——, "Vertical flight path and speed control autopilot design using total energy principles," in *Guidance and Control Conference*, 1983, p. 2239.

[9] F. Gavilan, J. Acosta, and R. Vazquez, "Control of the longitudinal flight dynamics of an UAV using adaptive backstepping," *IFAC Proceedings Volumes*, vol. 44, no. 1, pp. 1892–1897, 2011.

[10] A. Anandakumar, D. Bernstein, and A. Goel, "Adaptive energy control of longitudinal aircraft dynamics," in *AIAA SCITECH 2022 Forum*, 2022, p. 0965.

[11] E. Abdulhamitbilal, E. M. Jafarov, and M. Ş. Kavsaoğlu, "Matlab-simulink nonlinear modeling and simulation of aircraft longitudinal dynamics," in *Proc. of. Eurosim*, 2007.